Colloid Polym Sci (2007) 285:977–983
DOI 10.1007/s00396-007-1641-9

ORIGINAL CONTRIBUTION

A fluoroalkyl end-capped *N*-(1,1-dimethyl-3-oxobutyl) acrylamide oligomer/silica gel nanocomposite with no weight loss even at 800 °C equal to an original silica gel

Hideo Sawada · Tamikazu Narumi · Shun Kodama · Motohisa Kamijo · Ryou Ebara · Masashi Sugiya · Yasukazu Iwasaki

Received: 23 August 2006 / Accepted: 26 December 2006 / Published online: 8 February 2007

Abstract Fluoroalkyl end-capped *N*-(1,1-dimethyl-3-oxobutyl)acrylamide oligomer [R_F-(DOBAA)$_n$-R_F]/silica gel nanocomposite, which was prepared by reaction of the corresponding fluorinated oligomer with tetraethoxysilane and silica gel nanoparticles under alkaline conditions, exhibited no weight loss even at 800 °C equal to the original silica gel, although the corresponding parent R_F-(DOBAA)$_n$-R_F oligomer was completely degraded at 600 °C. Thermogravimetric analyses/mass spectra of fluorinated nanocomposite showed that this nanocomposite decomposed around 280 °C to afford CO_2 and H_2O as the major evolved gaseous products including some minor fluoro- and hydrocarbons. X-ray photoelectron spectroscopy analyses also showed that the contents of C, F, and Si atoms in R_F-(DOBAA)$_n$-R_F/SiO_2 nanocomposite after the calcination at 800 °C were similar to those before the calcination. These findings suggest that the evolved gaseous products should be encapsulated quantitatively into nanometer-size-controlled silica matrices to give the fluorinated silica gel nanocomposite with no weight loss even at 800 °C equal to the original silica gel.

Keywords Fluorinated oligomer · Silica gel · Nanocomposite · No weight loss · TG/Mass · XPS

H. Sawada (✉) · T. Narumi · S. Kodama
Department of Frontier Material Chemistry,
Faculty of Science and Technology,
Hirosaki University,
Bunkyo-cho,
Hirosaki 036-8561, Japan
e-mail: hideosaw@cc.hirosaki-u.ac.jp

M. Kamijo · Y. Iwasaki
Nissan Research Center, Nissan Motor Co., Ltd.,
Yokosuka-shi, Kanagawa 237-8523, Japan

R. Ebara · M. Sugiya
Research and Development Division,
Nippon Chemical Industrial Co., Ltd.,
Koto-ku,
Tokyo 136-8515, Japan

Introduction

There have been much attractive attention in advanced hybrid organic–inorganic composites because of exhibiting a large variety of extraordinary characteristics deriving from the synergism between the properties of each individual material [1–3]. The most commonly employed preparative procedures for these organic–inorganic hybrids are based on the sol–gel process, which leads to the formation of the inorganic network by starting from liquid precursors such as metal alkoxides and organic polymers preferably with suitable reactive groups [4–7]. A great interest has also been focused on the studies involving hybrids based on blends of oxides such as silica and organic polymers dispersed well at molecular levels [8, 9]. In general, the thermal stability of these organic–inorganic composites decreases extremely compared to that of the corresponding parent inorganic materials because of the presence of organic polymers in the composites. Fluorinated polymers such as poly(tetrafluoroethylene), poly(vinylidene fluoride), and perfluoropolyether are attractive functional materials because of exhibiting a variety of unique characteristics such as excellent chemical and thermal stability, low surface energy, and low refractive index and dielectric constant, which cannot be achieved from the corresponding nonfluorinated ones [10–22]. Therefore, from the developmental viewpoints of novel high-performance thermally

resistant materials, hybridizations of these fluorinated polymers with metal alkoxides are in particular interest, and in fact, some studies on the hybridization of fluorinated polymers with alkoxysilanes have been hitherto reported. However, the thermal stability of these hybrids are, in general, inferior to that of the original silica gels [23–26]. In this paper, we report a fluoroalkyl end-capped oligomer/silica gel nanocomposite (mean diameter, 36 nm) with no weight loss even at 800 °C equal to the original silica gel: This material has been prepared by reaction of fluoroalkyl end-capped *N*-(1,1-dimethyl-3-oxobutylacrylamide) oligomer [R_F-(DOBAA)$_n$-R_F] with tetraethoxysilane (TEOS) and nanosilica gel (mean diameter, 11 nm) under alkaline conditions [27]. In contrast, the weight of fluoroalkyl end-capped acrylic acid oligomer in fluoroalkyl end-capped acrylic acid oligomer/silica gel nanocomposite markedly dropped around 250 °C and decomposed gradually, reaching 0% around 540 °C.

Results and discussion

The reaction schemes for the preparation of these fluoroalkyl end-capped oligomers/silica gel composites were illustrated in Scheme 1.

Elementary analyses of fluorines in R_F-(DOBAA)$_n$-R_F/SiO_2 and R_F-(ACA)$_n$-R_F/SiO_2 nanocomposites in Scheme 1 showed that the contents of fluoroalkyl end-capped oligomers in these nanocomposites were estimated to be 23 and 22%, respectively. We have measured the size of these fluorinated oligomers–silica nanocomposite in methanol by dynamic light-scattering (DLS) measurements at 25 °C. Fluorinated oligomers/silica gel composites were nanometer-size-controlled particles (36.2 and 31.0 nm; see Scheme 1) with good dispersibility and stability in a variety of solvents including water. The transmission electron micrograph (TEM) of R_F-(DOBAA)$_n$-R_F/SiO_2 composites also showed the formation of fluorinated oligomer/SiO_2 composite with a mean diameter of 59 nm (see Fig. 1). The difference in the average sizes determined by DLS and TEM (DLS, ~36 nm; TEM, ~59 nm) would be due to the coagulation or agglomeration of the nanoparticles during sample preparation for TEM measurements. In addition, the specific surface area and particle size of R_F-(DOBAA)$_n$-R_F/SiO_2 composites were determined by the Brunauer-Emmett-Teller method [28], and the results were 134 m^2/g and 99 nm, respectively, indicating the nanoparticle characteristic.

Thermal stability of these fluorinated oligomers/silica gel nanocomposites was studied by the use of thermogravimetric analyses (TG) in which the weight loss of these nanocomposites was measured by raising the temperature around 800 °C (the heating rate, 10 °C/min) in air atmosphere, and the results were shown in Figs. 2 and 3.

As shown in Fig. 2, the weight of parent R_F-(ACA)$_n$-R_F oligomer markedly dropped around 250 °C and decomposed gradually, reaching 0% around 540 °C. A similar tendency was observed in R_F-(ACA)$_n$-R_F/SiO_2 nanocomposite, and a constant value for its weight loss was observed above 540 °C, indicating that this nanocomposite could possess silica gel nanoparticles. The content of parent R_F-(ACA)$_n$-R_F oligomer in this nanocomposite was estimated to be 26% by using these TG data, and this finding is quite similar to the obtained value (22%) by the elementary analyses of fluorine. On the other hand, as shown in Fig. 3, unexpectedly, we could not observe the weight loss of R_F-(DOBAA)$_n$-R_F oligomers/SiO_2 nanocomposite at all from room temperature to 800 °C equal to the original silica gel, although the parent R_F-(DOBAA)$_n$-R_F oligomer lost 100% of its weight at 600 °C. It was found that R_F-(DOBAA)$_n$-R_F oligomer/SiO_2 nanocomposite lost only 6% of their weight at 800 °C, which is the same value to that of the original silica gel. This finding indicates that pyrolytic fragments of R_F-(DOBAA)$_n$-R_F oligomer should be encapsulated effec-

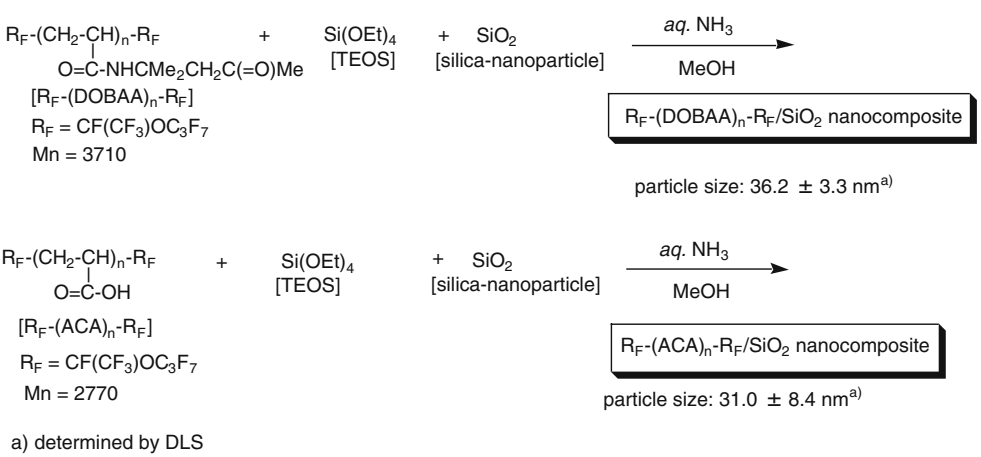

Scheme 1 The reaction schemes for the preparation of fluoroalkyl end-capped oligomers/silica gel composites

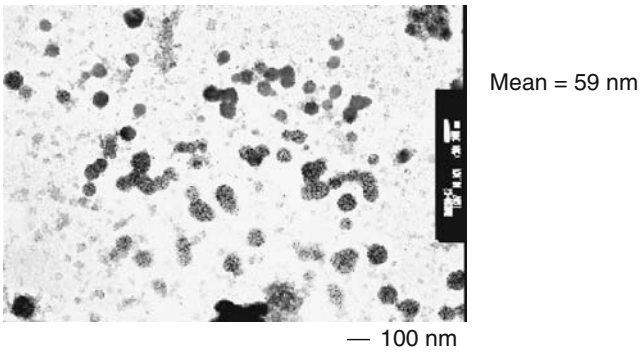

Fig. 1 TEM image of R_F-$(DOBAA)_n$-R_F/SiO_2 nanocomposite

tively into silica gel matrices. In addition, the average particle size (37.1±4.8 nm [determined by DLS]) of R_F-$(DOBAA)_n$-R_F oligomer/SiO_2 nanocomposite after the calcination was almost the same as that (36.2±3.3 nm) before the calcination and exhibited a good dispersibility and stability in a variety of solvents.

Differential thermal analyses for the R_F-$(DOBAA)_n$-R_F/SiO_2 nanocomposites in air atmosphere (the heating rate, 10 °C/min) showed that as the temperature reached around 250 °C, the exothermic phenomenon occurred (lasted till around 400 °C), and the weak exothermic peak appeared at 307 °C, which may be caused by the decomposition of R_F-$(DOBAA)_n$-R_F oligomer in the composite (see Fig. 4). A similar result was obtained in the case of the parent R_F-$(DOBAA)_n$-R_F oligomer (data not shown). Thus, the pyrolysis of R_F-$(DOBAA)_n$-R_F oligomer in the nanocomposite should occur around 307 °C to afford the pyrolytic fragments derived from this oligomer. On the other hand, during the calcination process of R_F-$(ACA)_n$-R_F/SiO_2 nanocomposite, two obvious exothermic peaks were observed at 396 and 503 °C, respectively (see Fig. 4).

To clarify the pyrolytic fragments derived from R_F-$(DOBAA)_n$-R_F oligomer/SiO_2 nanocomposite, the evolved

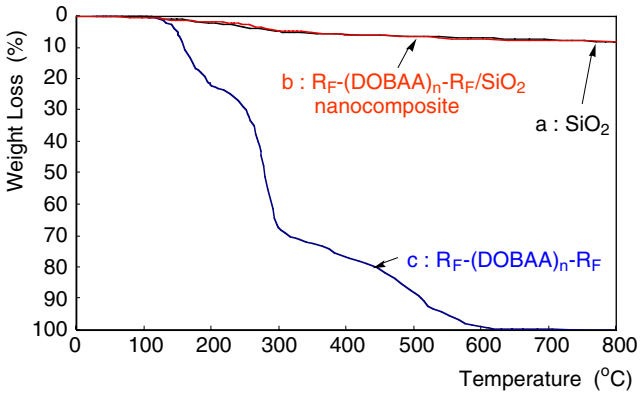

Fig. 3 Thermogravimetric analyses of R_F-$(DOBAA)_n$-R_F/SiO_2 nanocomposite [R_F=$CF(CF_3)OC_3F_7$]. *a: SiO_2, b: R_F-$(DOBAA)_n$-R_F/SiO_2-nanocomposite, c: R_F-$(DOBAA)_n$-R_F*

gases during TG measurements were analyzed by using a TG/Mass apparatus (Bruker AXS, TG-DTA2020SA/MS9610, Japan; the heating rate,10 °C/min) under the mixed gas atmosphere of helium (80%) and oxygen (20%). The parent R_F-$(DOBAA)_n$-R_F oligomer was also measured under similar conditions, for comparison. These results were shown in Figs. 5 and 6.

As shown in Fig. 5, the in situ nanocomposite produced H_2O and CO_2 around 290 °C as the major products with a minor product (HF), corresponding to the slight changes in TG illustrated in Fig. 3. A similar result was obtained in the case of the parent R_F-$(DOBAA)_n$-R_F oligomer (see Fig. 6). From the peak areas of H_2O and CO_2 in Figs. 5 and 6, we have estimated the amounts of encapsulated H_2O and CO_2 into the silica gel matrices based on the amounts of completely evolved H_2O and CO_2 in the pyrolysis of the parent R_F-$(DOBAA)_n$-R_F oligomer. The amounts of the encapsulated H_2O and CO_2 into silica gel matrices were 65 and 72%, respectively, and the product yield ratio of H_2O/

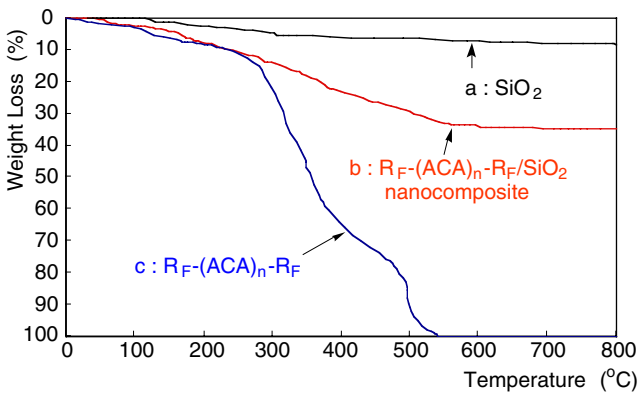

Fig. 2 Thermogravimetric analyses of R_F-$(ACA)_n$-R_F/SiO_2 nanocomposite [R_F=$CF(CF_3)OC_3F_7$]. *a: SiO_2, b: R_F-$(ACA)_n$-R_F/SiO_2nanocomposite, c: R_F-$(ACA)_n$-R_F*

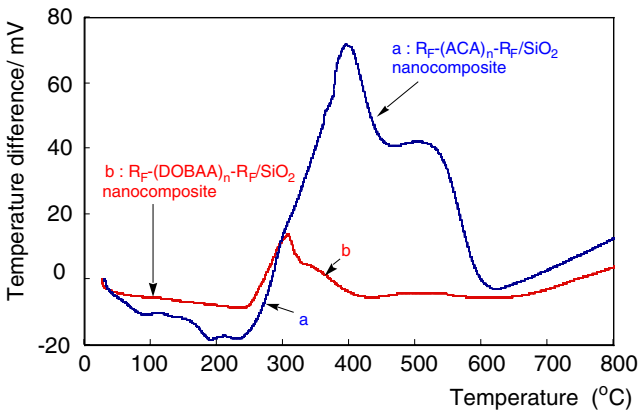

Fig. 4 Differential thermal analyses of of R_F-$(ACA)_n$-R_F/SiO_2 and R_F-$(DOBAA)_n$-RF/SiO_2 nanocomposites [R_F=$CF(CF_3)OC_3F_7$]. *a: R_F-$(ACA)_n$-R_F/SiO_2nanocomposite, b: R_F-$(DOBAA)_n$-R_F/SiO_2nanocomposite*

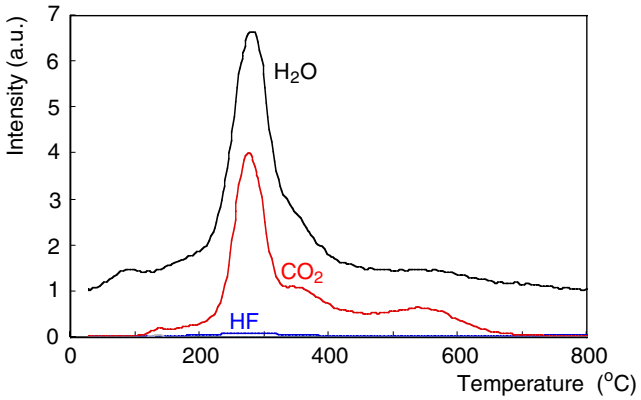

Fig. 5 TG/Mass spectra of R_F-$(DOBAA)_n$-R_F/SiO_2 nanocomposite [R_F=$CF(CF_3)OC_3F_7$]

CO_2 is 1.48. Some trace amounts of gaseous products such as HF, fluorocarbons ($C_2F_3OC_3F_7$, pentafluoroethane), and hydrocarbons (terahydrofuran, methylcyclopentenone, butanedione monooxime, and nitroethane) were also detected as by-products.

Figure 7 shows the X-ray diffraction (XRD) patterns of the original R_F-$(DOBAA)_n$-R_F/SiO_2 nanocomposite at room temperature and the samples heated in air atmosphere from room temperature to 800 °C. We had the same diffraction intensities and one broad peak around 22 degrees in each temperature, indicating that silica gel matrices could not be changed at all by the interaction with R_F-$(DOBAA)_n$-R_F oligomer under these conditions.

We have measured elementary analyses of carbon and hydrogen for R_F-$(DOBAA)_n$-R_F/SiO_2 nanocomposite before and after the calcination at 800 °C, and the results were as follows:

before calcination	carbon : 3.63%	hydrogen : 0.73%
after calcination	carbon : 0%	hydrogen : 0.20%

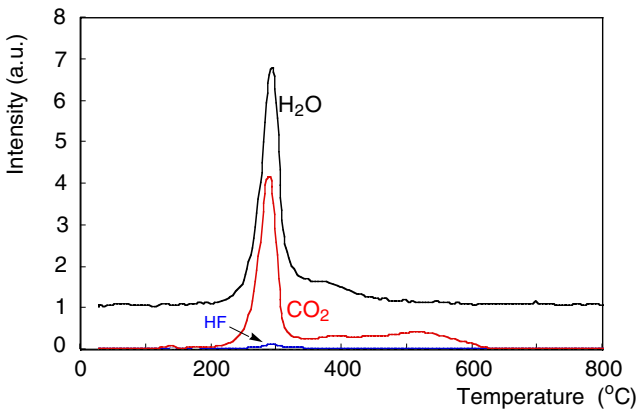

Fig. 6 TG/Mass spectra of R_F-$(DOBAA)_n$-R_F oligomer [R_F=$CF(CF_3)OC_3F_7$]

We cannot at all detect the content of carbon after the calcination. To clarify the presence of carbon, oxygen, fluorine, and silicon after the calcination at 800 °C, we analyzed the R_F-$(DOBAA)_n$-R_F/SiO_2 nanocomposite after the calcination at 800 °C by the use of X-ray photoelectron spectroscopy (XPS: Shimadzu ESCA-3400, Kyoto, Japan) technique, and the elementary atomic compositions [carbon (C_{1s}), fluorine (F_{1s}), oxygen (O_{1s}), and silicon (Si_{2p})] of this composite were estimated. We have also measured the elementary atomic compositions of R_F-$(ACA)_n$-R_F/SiO_2 silica gel nanocomposite by XPS technique under similar conditions, for comparison. These results were shown in Table 1.

As shown in Table 1, very interestingly, the contents of C, F, and Si atoms in R_F-$(DOBAA)_n$-R_F/SiO_2 nanocomposite after the calcination exhibited similar values to those before the calcination. However, in the case of R_F-$(ACA)_n$-R_F/SiO_2 nanocomposite after the calcination, the contents of C and F atoms were found to decrease extremely compared to those before the calcination. The content of Si atom in R_F-$(DOBAA)_n$-R_F/SiO_2 nanocomposite exhibited the similar value in the cases before and after the calcination; however, the content of O atom was found to increase slightly after the calcination. On the other hand, the contents of Si and O atoms in R_F-$(ACA)_n$-R_F/SiO_2 nanocomposite increased remarkably after the calcination, indicating that R_F-$(ACA)_n$-R_F oligomer in the nanocomposite has been completely consumed during the calcination process. In these composites, we could not detect the nitrogen atoms quantitatively by XPS technique because of their trace amount formations. These findings suggest that pyrolytic products such as CO_2 and H_2O derived from R_F-$(DOBAA)_n$-R_F oligomer in the nanocomposite should be encapsulated quite effectively into the nanometer-size-controlled silica matrices through the calcination process, because molecular-level combination, which is due to the strong interaction between the amido or carbonyl groups in fluoroalkyl end-capped oligomer and residual silanol groups through the intermolecular hydrogen bonding, should be essential for the architecture of the novel host moieties for the encapsulation of the evolved gaseous products into the silica matrices during the calcination process. Therefore, in the case of R_F-$(ACA)_n$-R_F/SiO_2 nanocomposites, such molecular-level combination could not be participated in the silica matrices because of the absence of amido and carbonyl groups in oligomer. Recently, we have reported that micrometer-size-controlled R_F-$(DOBAA)_n$-R_F/SiO_2 composites have a lower thermal stability compared to that of the original silica gel, and parent R_F-$(DOBAA)_n$-R_F oligomer in these composites decomposed completely at 800 °C owing to their poor molecular-level combination at the architectures of these micrometer-size-controlled composites [29].

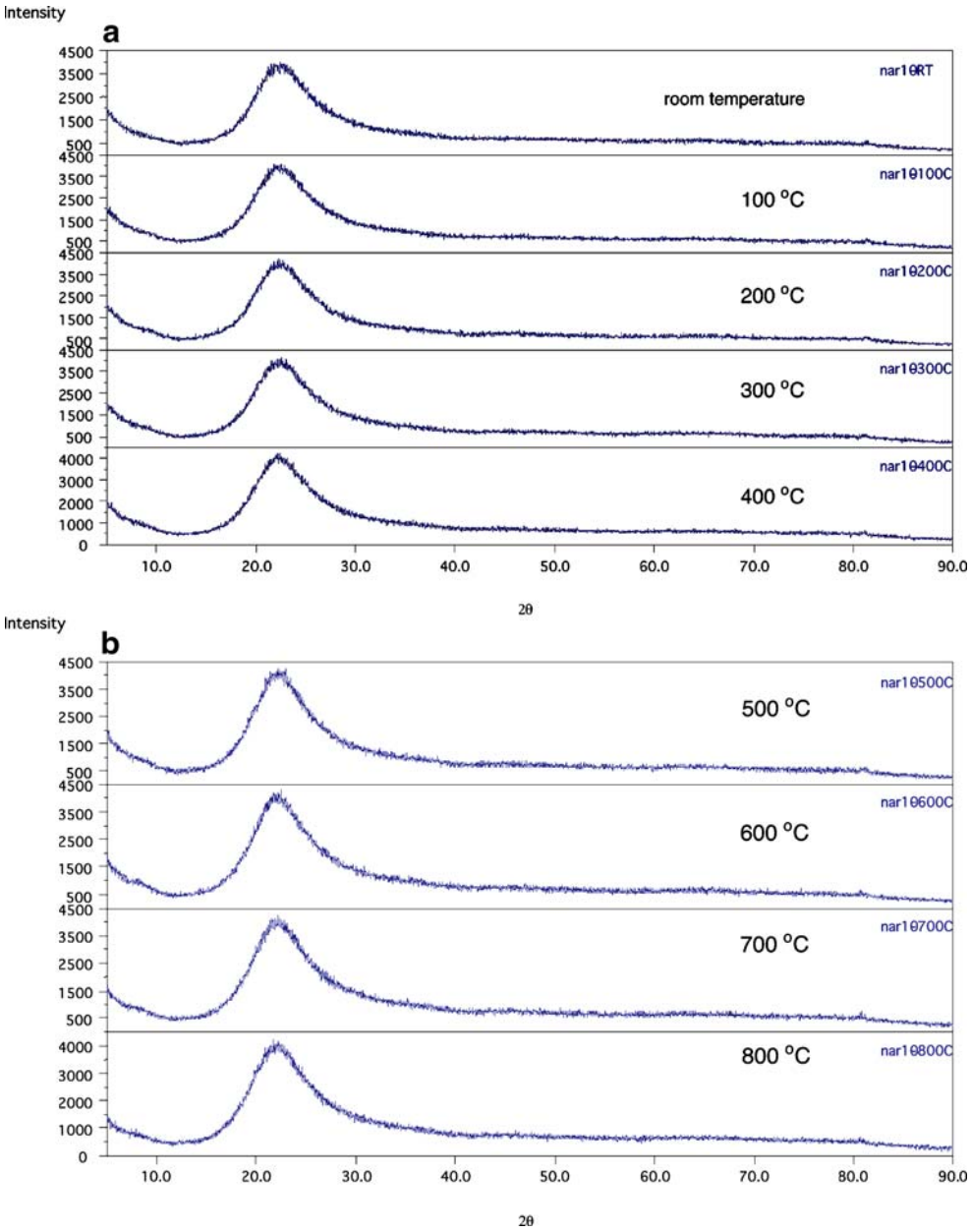

Fig. 7 **a** XRD patterns of R_F-$(DOBAA)_n$-RF/SiO_2 nanocomposite with the increase of heating temperature (from room temperature to 400 °C). **b** XRD patterns of R_F-$(DOBAA)_n$-R_F/SiO_2 nanocomposite with the increase of heating temperature (from 500 to 800 °C)

In addition, we have succeeded in preparing guest molecules such as ionic-liquids-encapsulated R_F-$(DOBAA)_n$-R_F/SiO_2 nanocomposites. Ionic liquids are well known to be nonvolatile and nonflammable [30]. In fact, as shown in Fig. 8, phosphonium salt-type ionic liquid $Bu_4P^+{}^-SP(=S)(OEt)_2$ is thermally stable, and its weight dropped around 250 °C. However, very interestingly, we could not at all observe the weight loss of this ionic-liquid-encapsulated R_F-$(DOBAA)_n$-R_F/SiO_2 nanocomposite (R_F=$CF(CF_3)OC_3F_7$, Mn [oligomer], 3,710; average particle size determined by DLS, 27.1 nm; content of R_F-$(DOBAA)_n$-R_F oligomer determined by elementary analyses of fluorine, 19%; the content of ionic liquid in this fluorinated nanocomposite determined by inductive coupled plasma analyses, 4%) from room temperature to 800 °C, and the weight loss ratio of this ionic-liquid-encapsulated nanocomposite became extremely lower compared to that of the original silica gel or R_F-$(DOBAA)_n$-R_F/SiO_2 nanocomposite (see Fig. 8). We have

Table 1 Elementary atomic compositions (%) by XPS analyses for R_F-$(D0BAA)_n$-R_F/SiO_2 and R_F-$(ACA)_n$-R_F/SiO_2 nanocomposites before and after the calcination at 800 °C

Composite	C_{1s}	F_{1s}	O_{1s}	Si_{2p}
R_F-$(D0BAA)_n$-R_F/SiO_2 nanocomposite				
Before calcination	10.67	4.98	55.57	28.78
After calcination	7.21	2.63	60.49	29.68
R_F-$(ACA)_n$-R_F/SiO_2 nanocomposite				
Before calcination	16.45	8.23	51.36	23.96
After calcination	2.60	1.08	66.01	30.31

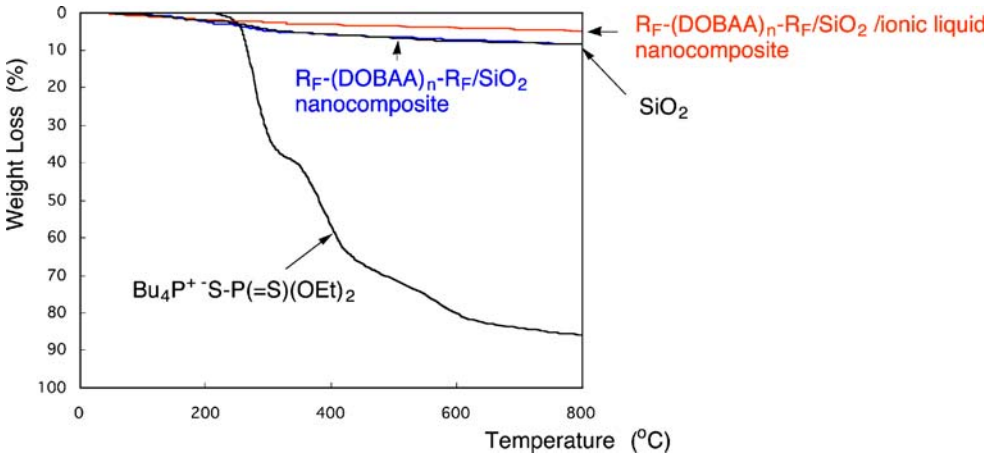

Fig. 8 Thermogravimetric analyses of R_F-(DOBAA)$_n$-R_F/SiO_2/ionic liquid nanocomposite [R_F=$CF(CF_3)OC_3F_7$]. SiO_2, R_F-(DOBAA)$_n$-R_F/SiO_2/ionic liquid nanocomposite, R_F-(DOBAA)$_n$-RF/SiO_2nanocomposite, ionic liquid: Bu_4P^{+-}S-P(=S)(OEt)$_2$

also prepared not only this ionic liquid but also other phosphorus-type ionic liquids such as $Bu_3P^+(C_8H_{17})$ $^-N(SO_2CF_3)_2$-, Bu_3P^+Me $^-OP(=O)(OMe)_2$-, $Bu_3P^+(C_8H_{17})$ PF_6^--, $(MeO)_3Si(CH_2)_3P^+(C_6H_{13})_3$ Cl^--, $Bu_3P^+(C_2H_2$-$CH_2OH)$ Cl^--, $Bu_3P^+(C_{12}H_{25})$ $^-OSO_2C_6H_3(CO_2Me)_2$-, and $Bu_3P^+(C_8H_{17})PF_4^-$-encapsulated R_F-(DOBAA)$_n$-R_F/SiO_2 nanocomposites under similar conditions, and a similar result with no weight loss was obtained in each nanocomposite. Therefore, it is strongly expected that our present technology is applicable to the development of the pyrolytic fragments derived from organic compounds to storage materials.

We find a unique fluoroalkyl end-capped *N*-(1,1-dimethyl-3-oxobutyl)acrylamide oligomer/SiO_2 nanocomposite with no weight loss even at 800 °C equal to the original silica gel. TG/Mass spectra of this fluorinated nanocomposite showed that the pyrolysis of this nanocomposite could afford H_2O and CO_2 as the major evolved gaseous products including some minor products. It was clarified that the evolved gaseous products (H_2O and CO_2) were encapsulated effectively into nanometer-size-controlled silica matrices with the encapsulated ratios 65 (H_2O) and 72% (CO_2) based on those of the parent R_F-(DOBAA)$_n$-R_F oligomer to give the fluorinated nanocomposite with no weight loss even at 800 °C equal to the original silica gel. XPS analyses showed that the contents of C, F, and Si atoms in R_F-(DOBAA)$_n$-R_F/SiO_2 nanocomposites after the calcination at 800 °C were similar to those before the calcination, indicating that the evolved gaseous products from the nanocomposites were encapsulated quite effectively into the silica matrices. Furthermore, we have succeeded in preparing guest molecules such as ionic-liquids-encapsulated R_F-(DOBAA)$_n$-R_F/SiO_2 nanocomposites with no weight loss even at 800 °C. From the developmental viewpoints for storage materials, our new fluoroalkyl end-capped oligomer/silica gel nanocomposite has high potential for not only high-performance thermally fluorinated resistant materials, but also new storage materials for the pyrolytic fragments derived from organic compounds.

Experimental

Preparation of fluoroalkyl end-capped N-(1,1-dimethyl-3-oxobutyl)acrylamide oligomer/silica gel nanocomposite A methanol solution (20 ml) of fluoroalkyl end-capped *N*-(1,1-dimethyl-3-oxobutyl)acrylamide oligomer {R_F-[CH_2CHC(=O)$NHCMe_2CH_2C$(=O)Me]$_n$-R_F [R_F-(DOBAA)$_n$-R_F]; R_F=$CF(CF_3)OC_3F_7$; Mn=3,710 (0.50 g)}, which was prepared by the reaction of fluoroalkanoyl peroxide with the corresponding monomer according to our previously reported method [31], was added with TEOS (0.47 g), silica-nanoparticle methanol solution [30 wt.%, 3.33 g; average particle size, 11 nm (Methanol Silica-sol (TR): Nissan Chemical Industrials, Tokyo, Japan)], and 25% aqueous ammonia solution (0.50 ml). The mixture was stirred with a magnetic stirring bar at room temperature for 2 h. After the solvent was evaporated, the obtained crude products were added with methanol (25 ml). The methanol solution was stirred with magnetic stirring bar at room temperature for 2 days and then was centrifuged for 30 min. The expected fluorinated nanocomposite was easily separated from the methanol solution. Fluorinated nanocomposite powders thus obtained were dried in vacuo at 50 °C for 2 days to afford purified particle powders (1.00 g). Fluoroalkyl end-capped acrylic acid oligomer/silica gel nanocomposite and ionic-liquids-encapsulated R_F-(DOBAA)$_n$-R_F/SiO_2 nanocomposites were also prepared under similar conditions.

Acknowledgement We thank S. Nagasawa (Bruker AXS. K. K., Japan) for TG/Mass observation and Y. Yoshida (Kratos Analytical, Japan) for XPS observation. This work was partially supported by a grant-in-aid for Scientific Research from the Ministry of Education, Science, Sports and Culture, Japan.

References

1. Judeinstein P, Sanchez C (1996) J Mater Chem 6:511–525
2. Wen J, Wilkes GL (1996) Chem Mater 8:1667–1681
3. Laine RM, Sanchez C, Brinker CJ, Giannelis E (1998) Organic–inorganic hybrid materials. Materials Research Society, Warrendale, PA, USA
4. Brinker CJ, Scherer GW (1990) Sol–gel science. Academic, Boston
5. Misra M, Guest A, Tilley M (1998) Surf Coat Int 81:594–595
6. Hua Z, Qiu K-Y (1997) Polymer 31:521–526
7. Pedroso MAS, Dias ML, San Gil RAS, Mothe CG (2003) Colloid Polym Sci 281:19–26
8. Matejka L, Plestil J (1997) Macromol Symp 122:191–196
9. Juangvanich N, Maurite KA (1998) J Appl Polym Sci 67:1799–1810
10. Johns K, Stead G (2000) J Fluorine Chem 104:5–18
11. Ameduri B, Boutevin B (2000) J Fluor Chem 104:53–62
12. Berret J-F, Calvet D, Collet A, Viguier M (2003) Curr Opin Colloid Interface Sci 8:296–306
13. Kujawa P, Goh CCE, Calvet D, Winnik FM (2001) Macromolecules 34:6387–6395
14. Imae T (2003) Curr Opin Colloid Interface Sci 8:307–314
15. Andruzzi L, Chiellini E, Galli G, Li X, Kang SH, Ober CK (2002) J Mater Chem 12:1684–1692
16. Imae T, Tabuchi H, Funayama K, Sato A, Nakamura T, Amaya N (2000) Colloid Surf A Physicochem Eng Asp 167:73–81
17. Jankova K, Hvilsted S (2005) J Fluorine Chem 126:241–250
18. Lebreton P, Ameduri B, Boutevin B, Corpart J-M (2002) Macromol Chem Phys 203:522–537
19. Sawada H (1996) Chem Rev 96:1779–1808
20. Sawada H, Kawase T (2001) Kobunshi Ronbunshu 58:147–160
21. Sawada H, Kawase T (2001) Kobunshi Ronbunshu 58:255–266
22. Sawada H (2000) J Fluorine Chem 105:219–220
23. Harmer MK, Farneth WE, Sun Q (1996) J Am Chem Soc 118:7708–7715
24. Cho J-W, Sul K-I (2001) Fiber Polym 2:135–140
25. Yano S, Okubo N, Takahashi K (1996) Macromol Symp 108:270–289
26. Fabbri P, Messori M, Montecchi M, Nannarone S, Pasquali L, Pilati F, Tonelli C, Toselli M (2006) Polymer 47:1055–1062
27. Sawada H, Narumi T, Kajiwara A, Ueno K, Hamazaki K (2006) Colloid Polym Sci 284:551–555
28. Gregg SJ, Sing KS, Sing W (1982) Adsorption, surface areas and porosity, 2nd edn. Academic, New York
29. Sawada H, Koizumi M, Tojo T, Ohnishi T, Tomoita T (2005) Polym Adv Technol 16:459–465
30. Welton T (1999) Chem Rev 99:2071–2084
31. Sawada H, Yoshino Y, Kurachi M, Kawase T, Takishita K, Tanedani T (2000) Polymer 41:397–4000